IOPscience iopscience.iop.org

Home Search Collections Journals About Contact us My IOPscience

Electronic and hydrogenic impurity states in a corner under an applied electric field

This article has been downloaded from IOPscience. Please scroll down to see the full text article.

1997 J. Phys.: Condens. Matter 9 1241

(http://iopscience.iop.org/0953-8984/9/6/010)

View the table of contents for this issue, or go to the journal homepage for more

Download details:
IP Address: 171.66.16.207
The article was downloaded on 14/05/2010 at 08:02

Please note that terms and conditions apply.

J. Phys.: Condens. Matter **9** (1997) 1241–1248. Printed in the UK PII: S0953-8984(97)71880-0

Electronic and hydrogenic impurity states in a corner under an applied electric field

Haiyang Zhou†‡ and Zhen-Yan Deng†§

† China Centre of Advanced Science and Technology (World Laboratory), PO Box 8730, Beijing 100080, People's Republic of China

‡ Department of Physics, Shanghai University, 149 Yanchang Road, Shanghai 200072, People's Republic of China

§ Shanghai Institute of Ceramics, Chinese Academy of Sciences, Shanghai 200050, People's Republic of China‖

Received 12 February 1996, in final form 13 November 1996

Abstract. With the use of a variational method to solve the effective-mass equation, we have studied the electronic and hydrogenic impurity states in a corner under an applied electric field. The electron energy levels and the impurity binding energies are calculated. Our results show that, with the increasing strength of the electric field, the electron energy levels increase, and the impurity binding energy in the ground state increases at first, to a peak value, then decreases to a value which is determined by the impurity position in the corner. The dependence of the impurity binding energy on the applied electric field and impurity position is discussed in detail.

1. Introduction

With the advances in the technology of molecular beam epitaxy (MBE), it is possible to fabricate quantum wells and quantum wires [1]. The interfaces in these structures play a significant role in determining the electronic and optical properties, and step structures usually exist at the interfaces [2–7], which affect the optical transition spectra considerably. Tanaka and Sakaki [5] and Tsuchiya *et al* [6] studied $Ga_{1-x}Al_xAs/GaAs$ quantum wells with periodic stepped interfaces and observed a strong optical anisotropy, which is attributed to the interface step structures. By angle-resolved photoelectron spectroscopy, Namba *et al* [8] studied the Ni(7 9 11) surfaces and found that a surface local state existed at the step edges on Ni(7 9 11) surfaces. In fact, a stepped surface or V-shaped groove of large size in an interface can be viewed as a corner; this model has been adopted by Lee and Antoniewicz [9] in studying the surface bound states and surface polaron states.

In quantum wells and quantum wires, the hydrogenic impurity states and the impurity binding energies have been studied extensively [10–16]. With the use of a variational method, similar to that used in the study of quantum wells [10], Brown and Spector [11] calculated the binding energies of hydrogenic impurity states in cylindrical quantum wires using infinite and finite cylindrical confining potentials for arbitrary impurity positions. Their results showed that for the infinite-potential-well model, the binding energy continues to increase as the radius of the wire decreases, while in the finite-potential-well model, the binding energy reaches a peak value as the wire radius decreases and then decreases

‖ Mailing address.

0953-8984/97/061241+08$19.50 © 1997 IOP Publishing Ltd

to a value characteristic of the cladding. Bryant [12] studied the effects of changing the cross sectional form on the impurity binding energy in quantum wires. Branis *et al* [13] calculated the binding energy of a hydrogenic donor in cylindrical quantum wires in the presence of a magnetic field. Using the variational method [14], Chen *et al* [15] calculated the impurity binding energy in the ground state in a quantum well under an electric field, and Cao and Thoai [16] calculated the hydrogenic impurity binding energy in the ground state in a rectangular quantum wire under an electric field. Recently, Deng *et al* [17] studied the electronic and shallow impurity states in a right-angled corner by considering the dielectric mismatch between the well material and the barrier material. The results showed that the binding energy of the impurity ground state tends to the value of the third impurity excited state in the bulk when the impurity approaches the corner.

In this paper, we investigate the electronic and hydrogenic impurity states in a corner made by two orthogonal surfaces under an applied electric field. Because the electric field pushes the electrons towards the corner, the electron motion is quantized in the lateral direction, but it is free along the longitudinal direction, like the electron behaviour in quantum wires. For the electronic states, we adopt the Airy function, while for the hydrogenic impurity states, we adopt a variational method.

The paper is organized as follows. In section 2, we study the electronic states. In section 3, we study the hydrogenic impurity states. The numerical results and discussion are presented in section 4.

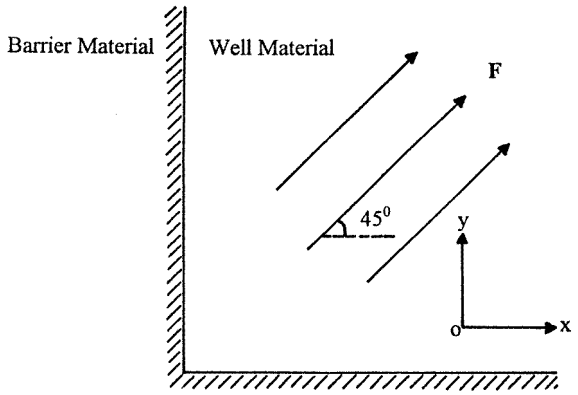

Figure 1. A schematic representation of a right-angled corner structure under an applied electric field, where the well material and barrier material are inside and outside of the corner, respectively.

2. Electronic states

Let us consider an electron moving in a right-angled corner structure with the well material inside the corner and the barrier material outside of the corner, as shown in figure 1. An electric field $\boldsymbol{F} = (1, 1, 0)(F/\sqrt{2})$ is applied along the diagonal line of the corner. In the effective-mass approximation, the Hamiltonian for electron states in the corner can be written as

$$H_0 = P^2/2m_b + V(\boldsymbol{r}) + eFx/\sqrt{2} + eFy/\sqrt{2} \tag{1}$$

where m_b is the electron band effective mass, and $\boldsymbol{r}$ and $\boldsymbol{p}$ are the electron coordinate and momentum, respectively. The electron-confining potential well in the corner is given by

$$V(\boldsymbol{r}) = \begin{cases} 0 & x > 0 \text{ and } y > 0 \\ \infty & \text{otherwise.} \end{cases} \tag{2}$$

Provided that the variables are separable, the electronic wavefunction for the Hamiltonian H_0 is written as

$$\begin{aligned} &\Phi(\boldsymbol{r}) = (N/\sqrt{L_z})\,\mathrm{Ai}(\xi)\,\mathrm{Ai}(\zeta)\exp(\mathrm{i}k_z z) \\ &\xi = x/l - \lambda_m \\ &\zeta = y/l - \lambda_n \\ &l = [\hbar^2/\sqrt{2}m_b eF]^{1/3} \end{aligned} \tag{3}$$

where N and L_z are the normalization coefficients, l is the electron characteristic length under the electric field, λ_m and λ_n are dimensionless constants, and $\mathrm{Ai}(\xi)$ is the Airy function which is defined by [18]

$$\mathrm{Ai}(\xi) = \begin{cases} \frac{1}{3}\sqrt{|\xi|}[J_{1/3}(\frac{2}{3}|\xi|^{3/2}) + J_{-1/3}(\frac{2}{3}|\xi|^{3/2})] & \xi < 0 \\ (1/\pi)\sqrt{\xi/3}K_{1/3}(\frac{2}{3}|\xi|^{3/2}) & \xi > 0 \end{cases} \tag{4}$$

where $J_{1/3}$ is the Bessel function of order 1/3, and $K_{1/3}$ is the modified Bessel function of the second kind of order 1/3. The electronic wavefunction $\Phi(\boldsymbol{r})$ satisfies the following boundary conditions:

$$\Phi(\boldsymbol{r})|_{x=0} = \Phi(\boldsymbol{r})|_{y=0} = 0 \tag{5a}$$

which are equivalent to

$$\mathrm{Ai}(-\lambda_n) = \mathrm{Ai}(-\lambda_m) = 0 \tag{5b}$$

where $m, n = 1, 2, 3, \ldots$ are positive integers, $\lambda_{m(n)}$ is the zero point of the Airy function, and $\lambda_1 = 2.388$. The electron energy levels are given by

$$E_{mn} = [\hbar^2/2m_b l^2](\lambda_m + \lambda_n) + \hbar^2 k_z^2/2m_b. \tag{6}$$

The electronic wavefunction in the ground state is

$$\begin{aligned} &\Phi_0(\boldsymbol{r}) = (N/\sqrt{L_z})\,\mathrm{Ai}(\xi)\,\mathrm{Ai}(\zeta)\exp(\mathrm{i}k_z z) \\ &\xi = x/l - \lambda_1 \\ &\zeta = y/l - \lambda_1 \end{aligned} \tag{7}$$

and the electron energy in the ground state is

$$E_0 = \hbar^2\lambda_1/m_b l^2 + \hbar^2 k_z^2/2m_b. \tag{8}$$

3. Impurity states

When the impurity is placed at the position $\boldsymbol{r}_0 = (x_0, y_0, 0)$ inside the corner, the Hamiltonian for the impurity states can be written as

$$H(\boldsymbol{r}) = P^2/2m_b + V_{\mathrm{ion}}(\boldsymbol{r}) + V(\boldsymbol{r}) + eFx/\sqrt{2} + eFy/\sqrt{2} \tag{9}$$

where

$$V_{\mathrm{ion}}(\boldsymbol{r}) = -e^2/(\varepsilon|\boldsymbol{r} - \boldsymbol{r}_0|) \tag{10}$$

and ε is the dielectric constant of the well material. Like in the case of quantum wells [10] and quantum wires [11], we choose the trial wavefunction for the ground impurity state to be

$$\begin{aligned} &\psi(\boldsymbol{r}) = N(\beta)\,\mathrm{Ai}(\xi)\,\mathrm{Ai}(\zeta)\exp(-\beta|\boldsymbol{r}-\boldsymbol{r}_0|) \\ &\xi = x/l - \lambda_1 \\ &\zeta = y/l - \lambda_1 \end{aligned} \tag{11}$$

where $N(\beta)$ is the normalization constant, β is the variational parameter, and λ_1 is the first zero point of the Airy function. The above trial wavefunction satisfies the boundary conditions. $N(\beta)$ is given by

$$\begin{aligned} &N(\beta) = \left[\int_0^\infty \mathrm{d}x \int_0^\infty \mathrm{d}y\ \mathrm{Ai}^2(\xi)\,\mathrm{Ai}^2(\zeta)\,2|\boldsymbol{\rho}-\boldsymbol{\rho}_0|K_1(2\beta|\boldsymbol{\rho}-\boldsymbol{\rho}_0|)\right]^{-1/2} \\ &|\boldsymbol{\rho}-\boldsymbol{\rho}_0| = [(x-x_0)^2 + (y-y_0)^2]^{1/2}. \end{aligned} \tag{12}$$

The impurity ground-state energy is

$$\begin{aligned} \langle\psi|H(\boldsymbol{r})|\psi\rangle = {} & [\hbar^2\lambda_1/m_b l^2 + \hbar^2\beta^2/2m_b] + N^2(\beta)\int_0^\infty \mathrm{d}x \int_0^\infty \mathrm{d}y\ \left\{\frac{\hbar^2}{m_b l}\right. \\ & \times \left[\mathrm{Ai}(\xi)\,\frac{\mathrm{d}\,\mathrm{Ai}(\xi)}{\mathrm{d}\xi}\,\mathrm{Ai}^2(\zeta)\beta(x-x_0) + \mathrm{Ai}^2(\xi)\,\frac{\mathrm{d}\,\mathrm{Ai}(\zeta)}{\mathrm{d}\zeta}\,\mathrm{Ai}(\zeta)\beta(y-y_0)\right] \\ & \left. + (\hbar^2\beta/m_b - e^2/\varepsilon)\,\mathrm{Ai}^2(\xi)\,\mathrm{Ai}^2(\zeta)\right\} 2K_0(2\beta|\boldsymbol{\rho}-\boldsymbol{\rho}_0|) \end{aligned} \tag{13}$$

where K_0 and K_1 are the modified Bessel functions of the second kind of order 0 and 1, respectively.

The impurity binding energy E_b is defined as the energy difference between the bottom of the electronic conduction band without the impurity ($k_z = 0$) and the ground-state energy level of the impurity states in the corner:

$$E_b = E_0 - \min_\beta \langle\psi|H(\boldsymbol{r})|\psi\rangle. \tag{14}$$

4. Results and discussion

As an example, we choose $Ga_{1-x}Al_xAs/GaAs$ for numerical calculations [17]. For simplicity, the energy is in units of effective Rydbergs, $R^* = m_b e^4/2\hbar^2\varepsilon^2$, and the length is normalized to the effective Bohr radius $a_0^* = \hbar^2\varepsilon/m_b e^2$.

Figure 2 shows the dependence of the electron energy levels in the corner on the applied electric field. From figure 2, we can see that, with increasing strength of the electric field, the electron confined energies are enhanced. Because of the existence of the electric field, the electrons are confined in the corner, which is similar to the case where the electrons are confined in a quantum wire. Assuming that the ground electron energy level in the corner is equal to that in a square quantum wire:

$$\hbar^2\lambda_1/m_b l^2 = \hbar^2\pi^2/m_b d^2$$

where d is the width of quantum wire, we obtain the relationship of the equivalent width ($d_x = d_y$) of the quantum wire versus the applied electric field (F), as shown in figure 3. The results show that, with increasing strength of the electric field, the equivalent width of the square quantum wire decreases, indicating stronger confinement of electrons in the corner for the stronger electric field.

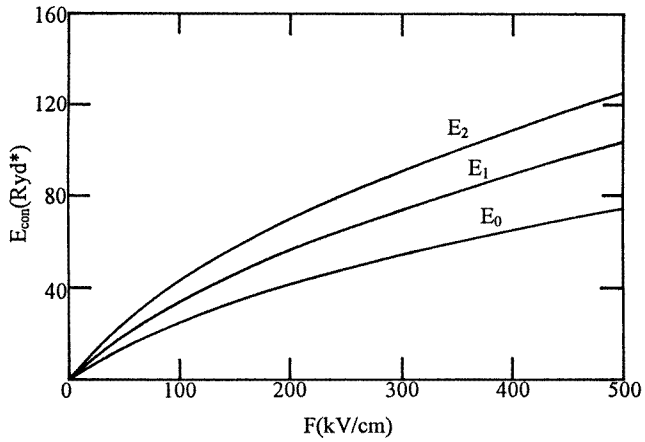

Figure 2. The electron confined energy levels versus the applied electric field. E_0, E_1 and E_2 represent the electron confined energy levels of the ground state, the first excited state, and the second excited state, respectively.

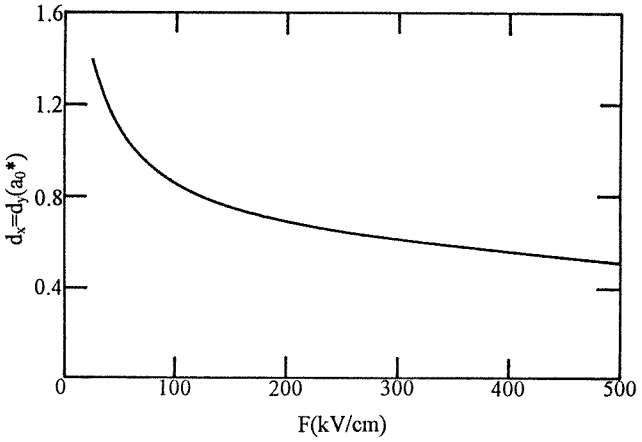

Figure 3. The equivalent width of a square quantum wire versus the applied electric field for the case where the ground electronic level in the corner is equal to that in the square quantum wire.

Figure 4 shows the ground impurity binding energy in the corner versus the electric field strength for different impurity positions. From figure 4, we can find that, when the impurity is at the corner ($x_0 = y_0 = 0$), with increasing strength of the electric field, the impurity binding energy increases monotonically; however, when the impurity is away from the corner, with increasing strength of the electric field, the impurity binding energy increases at first, to a peak value, then decreases to a value which is determined by the impurity position [11, 15]. For example, when the electric field value is considerable, the impurity binding energy is near to $\frac{1}{10}R^*$ for the impurity at $x_0 = y_0 = 10a_0^*$, as shown in figure 4. In order to show clearly the variation in impurity binding energy with electric field strength for the impurity at $x_0 = y_0 = 10a_0^*$ in the smaller-electric-field region in figure

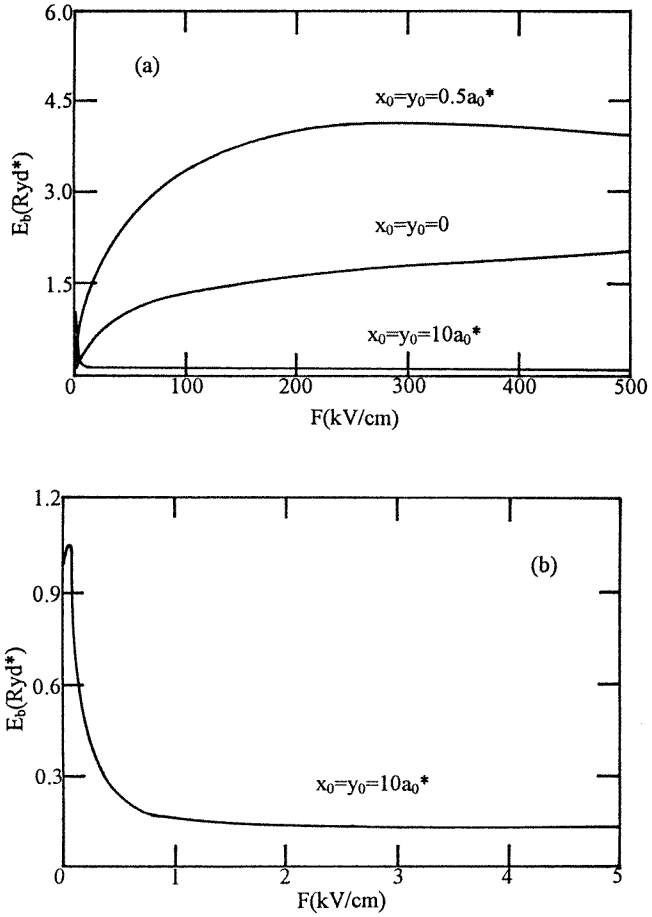

Figure 4. The ground impurity binding energy in the corner versus the electric field strength for different impurity positions: (a) the electric field strength ranges from 0 to 500 kV cm^{-1} for the impurity positions at $x_0 = y_0 = 0$, $x_0 = y_0 = 0.5a_0^*$, and $x_0 = y_0 = 10a_0^*$; and (b) the electric field strength ranges from 0 to 5 kV cm^{-1} for the impurity position at $x_0 = y_0 = 10a_0^*$.

4(a), we magnify this region, as shown in figure 4(b).

Figure 5 shows the ground impurity binding energy in the corner versus the impurity position for different electric fields. From figure 5, we can see that, when the electric field is not applied ($F = 0$), with increasing distance of the impurity away from the corner, the impurity binding energy increases from $0.11R^*$, and finally tends to $1R^*$ for $x_0 = y_0$ [17], and our result is $0.984R^*$, when $x_0 = y_0 = 10a_0^*$—see figure 5(a); while for $x_0 = 0$, it increases from $0.11R^*$, and finally tends to $\frac{1}{4}R^*$ [17], and our result is $0.243R^*$, when $x_0 = 0$ and $y_0 = 10a_0^*$—see figure 5(b). After the electric field is applied, with increasing distance of the impurity away from the corner, the impurity binding energy increases at first, to a peak value, then decreases monotonically. Moreover, as the applied electric field is enhanced, the peak value of the impurity binding energy becomes larger, and the impurity position corresponding to the peak value is nearer to the corner. These results are consistent with the variations in impurity binding energy with the sizes of the quantum wires [11, 15].

The results obtained above are interesting and their physical interpretation and discussion

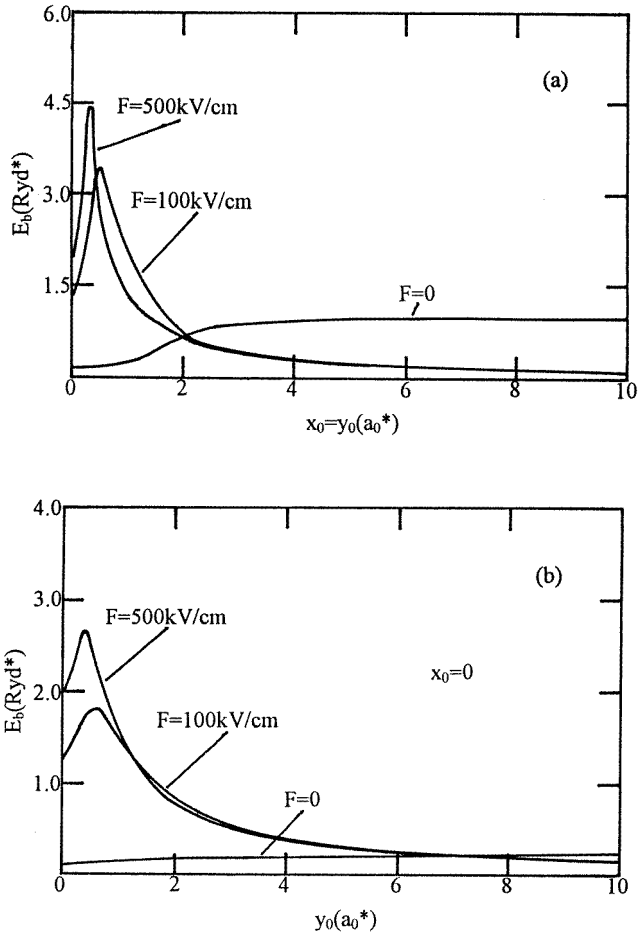

Figure 5. The ground impurity binding energy in the corner versus the impurity position for different electric fields: (a) $x_0 = y_0$; and (b) $x_0 = 0$.

are as follows. Because the electric field pushes the electrons towards the corner, the electrons in the well material are confined near the corner and the electron energy in the corner is quantized, like the electrons confined in a quantum wire. As the electric field strength increases, the confinement of the electrons in the corner is strengthened, and the electron energy levels in the corner increase, as shown in figure 2. As we know, the electron energy levels in a quantum wire increase with the decrease in its cross sectional size, and the equivalent width of the square quantum wire for the corner structure under an applied electric field decreases with the increase in the electric field strength, as shown in figure 3. The impurity behaviour in the corner structure under the applied electric field is also like the impurity behaviour in a quantum wire, due to the confinement of electrons in the corner. When the impurity is at the position $x_0 = y_0 = 0$ in the corner, it is equivalent to an impurity located at the corner point of a square quantum wire, and the impurity binding energy increases monotonically with the increase in the electric field strength, like in the case where the impurity binding energy at the corner point of a square quantum wire increases monotonically with the decrease in its cross sectional size [19, 20]. When the

impurity is not at the corner point, such as when the impurity position is at $x_0 = y_0 = 0.5a_0^*$ and $x_0 = y_0 = 10a_0^*$ as discussed near figure 4, the impurity position relative to the centre of the equivalent square quantum wire is changeable as the electric field strength varies; that is, the impurity position can move through the centre of the equivalent square quantum wire with the increase in the electric field strength. It is well known that the impurity position in quantum wires corresponding to the maximum binding energy is at the centre of the quantum wires [19, 20]. That the impurity binding energy increases at first, to a peak value, then decreases to a lower value for the impurity position not at the corner point, as shown in figure 4, is a result of the variations in distance between the impurity and the centre of the equivalent square quantum wire with the electric field strength. When the electric field strength is fixed, this means that the equivalent width of the quantum wire is fixed. As the impurity position is changed from the corner point, then to the centre of the equivalent square quantum wire, and finally away from the quantum wire, the impurity binding energy increases at first, then reaches a peak value, and finally decreases monotonically, as shown in figure 5, which is in perfect agreement with the results for quantum wires [19, 20]. In fact, it is easier to fabricate a corner structure than to fabricate a quantum wire in the experiments, and our theoretical results may provide a new way of detecting and applying quantum confinement effects.

In conclusion, we have investigated the electronic and hydrogenic impurity states in a right-angled corner under an applied electric field. For the electronic states, we adopt the Airy function, while for the hydrogenic impurity states, we adopt a variational approach. Our results show that the electron and impurity-state behaviour in the corner structure under the applied electric field is similar to that in the quantum wires. We hope that our theoretical results will stimulate further experimental investigations.

References

[1] Gerohoni D, Weiner J S, Chu S N G, Baraff G A, Vandenberg J M, Pfeiffer L N, West K, Logan R A and Tanbun-Ek T 1990 *Phys. Rev. Lett.* **65** 1631
[2] Weisbuch C, Dingle R, Gossard A C and Weigmann W 1980 *J. Vac. Sci. Technol.* **17** 1128
[3] Fujiwara K, Kanamoto K and Tsukada N 1989 *Phys. Rev.* B **40** 9698
[4] Tanaka M and Sakaki H 1988 *Japan. J. Appl. Phys.* **27** L2025
[5] Tanaka M and Sakaki H 1989 *Appl. Phys. Lett.* **54** 1326
[6] Tsuchiya M, Gaines J M, Yan R H, Simes R J, Holtz P O, Coldren L A and Petroff P M 1989 *Phys. Rev. Lett.* **62** 466
[7] Khoo G S and Ong C K 1993 *J. Phys.: Condens. Matter* **5** 6507
[8] Namba H, Nakanishi N, Yamaguchi T and Kuroda H 1993 *Phys. Rev. Lett.* **71** 4027
[9] Lee W W and Antoniewicz P R 1989 *Phys. Rev.* B **40** 3352
Lee W W and Antoniewicz P R 1989 *Phys. Rev.* B **40** 9920
[10] Bastard G 1981 *Phys. Rev.* B **24** 4714
[11] Brown J W and Spector H N 1986 *J. Appl. Phys.* **59** 1179
[12] Bryant G W 1984 *Phys. Rev.* B **29** 6632
Bryant G W 1985 *Phys. Rev.* B **31** 7812
[13] Branis S V, Li G and Bajaj K K 1993 *Phys. Rev.* B **47** 1316
[14] Bastard G, Mendez E E, Chang L L and Esaki L 1983 *Phys. Rev.* B **28** 3241
[15] Chen H, Li X and Zhou S 1991 *Phys. Rev.* B **44** 6220
[16] Cao H T and Thoai D B T 1995 *Physica* B **205** 273
[17] Deng Z Y, Zhang H and Guo J K 1994 *J. Phys.: Condens. Matter* **6** 9729
[18] Landau L D and Lifshitz E M 1977 *Quantum Mechanics* (Oxford: Pergamon)
[19] Brum J A 1985 *Solid State Commun.* **54** 179
[20] Weber G, Schulz P A and Oliveira L E 1988 *Phys. Rev.* B **38** 2179